Self-Assembled Structures in Electrospun Poly(styrene-*block*-isoprene) Fibers

Vibha Kalra,[†] Prashant A. Kakad,[‡] Sergio Mendez,[†] Timur Ivannikov,[†] Marleen Kamperman,[§] and Yong Lak Joo*,[†]

School of Chemical and Biomolecular Engineering, Cornell University, Ithaca, New York 14853; Department of Textiles and Apparel, Cornell University, Ithaca, New York 14853; and Department of Materials Science and Engineering, Cornell University, Ithaca, New York 14853

Received December 10, 2005; Revised Manuscript Received May 29, 2006

ABSTRACT: Formation of various domain shapes in submicron scale fibers of poly(styrene-*block*-isoprene) (PS-*b*-PI) has been investigated via electrospinning. Monodisperse PS-*b*-PI block copolymers with 29 and 53 vol % of PI were synthesized using two-step anionic polymerization and were dissolved in tetrahydrofuran (THF). Solutions of block copolymer with varying concentrations in THF were electrospun, and fibers with average diameters from 200 nm to 5 μm were obtained. Small-angle X-ray scattering (SAXS) and transmission electron microscopy (TEM) studies revealed that cylindrical and lamellar morphology can be formed in electrospun fibers of 29% and 53% PI copolymers, respectively. We note that these domain structures in fibers are not as well developed as those in films possibly due to the short residence time and strong elongational deformation involved in the electrospinning process. For both systems we find that the *d* spacing in electrospun fibers is smaller than that in the cast film. This could also be attributed to the elongational deformation and fast solvent evaporation during electrospinning. The domain structures of electrospun fibers from the symmetric (53% PI) copolymer exhibit the influence of fiber morphology such as confinement and curvature due to its high molecular weight. More uniform domain structures in the fibers and increase in *d* spacing are observed after the annealing process.

Introduction

Fibers with submicron diameters have been a subject of intensive research due to their large surface area-to-mass ratio and are finding uses in filtration, protective clothing, and biomedical applications.[1] These nanofibers can be formed using a relatively simple electrospinning process where a polymer solution or melt is continuously drawn from a syringe needle by a strong electric field. While the strong extension of the viscoelastic jet continuously reduces its diameter, rapid evaporation of solvent solidifies it, producing ultrathin fibers. We refer the reader to recent reviews that elaborate on the versatility and promise of this emerging process.[2,3] Studies on electrospinning, however, have been limited to relatively simple polymeric systems. Casper et al.[4] studied the effect of humidity and molecular weight on pore size and distribution on the surface of electrospun polystyrene fibers. Nanofiber formation from complex systems including composites[5,6] and block copolymers[7−9] is now beginning to be studied.

Block copolymer solutions and melts are known to self-assemble into a variety of nanoscale morphologies including spheres, rods, micelles, lamellae, vesicle tubules, and cylinders[10,11] depending on the volume fraction and interaction parameter between different blocks. This phenomenon has been extensively studied for both solution and melt via theory,[12,13] experiments,[14−16] and simulations.[17−20] Numerous studies have focused on the effect of shear on self-assembly in block copolymers.[21] Harada et al.[22] obtained highly oriented microstructures in ABABA pentablock copolymer and ABA triblock copolymer using solution extrusion. They reported that the transverse lamellae orientation can be achieved by extruding ABABA pentablock copolymer at high shear rates. Studies on the effect of elongational deformation on block copolymer self-assembly have also been conducted in the past. Seguela et al.[23] studied elongational deformation mechanism of solution-cast films of polybutadiene-hydrogenated SBS block copolymer exhibiting lamellar morphology. They found that lamellae undergo necking and rupture at the yield point. They also reported a reduction in first-order Bragg spacing with increasing longitudinal draw ratio in the neck region. Pakula and coworkers[24] studied the extensional deformation behavior of styrene−butadiene−styrene block copolymer exhibiting cylindrical morphology. They presented a variety of deformation behaviors that occur when the oriented microdomain structure is deformed at various angles to its original orientation. They also found that rupture of domain structures takes place at high extension rates with some evidence of lower domain spacing. Shin et al.[25] studied the effect of cylindrical confinement on morphology of PS-*b*-PBD using nanoporous alumina membrane. The copolymer film was annealed at 125 °C for it to enter the pores via capillary action, and the temperature was kept fixed for 24 h to allow the formation of stable equilibrium structures. They found that due to the high degree of curvature imposed in a cylindrical confinement certain frustration of chain packing occurs at the interface forming stacked PS lamellar structures along the axis of the pore.

Our work focuses on the development of self-assembled structures during the formation of submicronscale fibers in the electrospinning process. To our knowledge, there are only a few publications that report on the microphase separation of nanofibers formed by electrospinning block copolymer solutions. Fong et al.[7] produced nanofibers from styrene−butadiene−styrene triblock copolymer solution by electrospinning. They observed weak and irregular microphase separation on the surface of electrospun fibers. They found that annealing of fibers allowed the phase domains to become larger. Ma et al.[8] recently produced superhydrophobic microphase-separated nanofibers

[†] School of Chemical and Biomolecular Engineering.
[‡] Department of Textiles and Apparel.
[§] Department of Materials Science and Engineering.
* Corresponding author. E-mail: ylj2@cornell.edu.

10.1021/ma052643a CCC: $33.50 © 2006 American Chemical Society
Published on Web 07/06/2006

from solution of poly(styrene-*block*-dimethylsiloxane) block copolymer blended with homopolymer PS in THF and dimethylformamide via electrospinning. They reported the formation of PDMS cylinders in PS matrix via TEM. Self-assembly of comb-shaped supermolecules, polystyrene-*block*-poly(4-vinylpyridine) (PS-*b*-P4VP(PDP)−pentadecylphenol(PDP), in electrospun fibers has also been studied.[9]

In this paper, we report the formation of self-assembled structures in PS-*b*-PI diblock copolymers of two different compositions. Our experiments are the first to report the structure development in fibers formed by electrospinning symmetric block copolymer solution which forms lamellar morphology. Although previous results have been reported for cylindrical morphology in electrospun fibers, unlike earlier results, we see clear microphase separation via TEM of microtomed sections and SAXS. Furthermore, results on the effect of annealing on fiber morphology have also been presented.

Experimental Method

Material Synthesis. Two different compositions of PS-*b*-PI diblock copolymers were synthesized and used in the electrospinning study. For the copolymer which we refer to as "IS29", the molecular weights of styrene and isoprene blocks were 32 and 13 kg/mol, respectively, resulting in a 29 vol % isoprene. For "IS53" copolymer, the PS and PI molecular weights were 74 and 68 kg/mol, respectively, giving a 53 vol % isoprene. The synthesis of monodisperse PS-*b*-PI block copolymers is accomplished using a two-step living anionic polymerization. *sec*-Butyllithium is used as an initiator to first polymerize styrene monomer anionically and then to initiate isoprene monomer with this living polystyrene to form a living PS-*b*-PI diblock copolymer. The polydispersity of the polymer obtained by gel permeation chromatography is 1.04−1.05.

Sample Preparation. PS-*b*-PI copolymers with two different compositions are dissolved in THF. High molecular weight of IS53 copolymer allowed the formation of fibers using 15−25 wt % solutions in THF. However, because of the relatively low molecular weight of IS29 copolymer, 30−40 wt % solutions were needed to spin nonbeaded fibers. In the electrospinning unit, block copolymer solution was fed at a constant flow rate of 0.02 mL/min to a syringe by a digitally controlled micropump (Harvard Apparatus, PHD 2000). The tip of the syringe was connected to a high-voltage supply (Gamma High Voltage Research, ES-30P), and fibers were spun at an electrical potential of 20 kV using a 24 gauge needle. The distance between the tip of the needle and the grounded collector was kept fixed at about 10 cm.

Characterization. Morphology of electrospun fibers was examined by scanning electron microscopy (SEM) (Leica 440). The structural study was performed through TEM (JEOL 1200EX) and SAXS (Bruker-Axs Nanostar System). In the TEM study electrospun fibers were microtomed at room temperature using a diamond knife. Microtomed fibers were stained with osmium tetroxide vapors (OsO_4). TEM images of both the section along the fiber axis and cross-section were taken using JEOL 1200EX at an accelerating voltage of 120 kV. SAXS data were collected in the 2θ range of 0.1°−4°, in steps of 0.02° and a scanning rate of 4 s per point.

Results and Discussion

Solutions of 30−40 wt % of IS29 and 15−25 wt % of IS53 copolymer in THF were electrospun, and fibers with average diameters from 200 nm to 5 μm were obtained. A typical scanning electron microscopy (SEM) image of electrospun fibers is shown in Figure 1.

IS29 Electrospun Fibers. IS29 PS-*b*-PI bock copolymer film was cast from a 10 wt % solution in THF. Both TEM (Figure 2d) and SAXS (Figure 3) studies on the cast film show the existence of hexagonally packed PI cylinders in a PS matrix. 30 wt % solution in THF of the same block copolymer was then electrospun using the processing conditions mentioned above. TEM images taken from a microtomed IS29 fiber (Figure 2) show some evidence of hexagonal PI cylinders. It is interesting to note that the size of the PI domains is very small as seen in Figure 2a,b. The possible explanation for largely disordered and short cylinders is the strong elongational deformation during the electrospinning process that causes necking and rupture of the PI cylinders as reported in the literature.[24,26] Because of the rapid solvent evaporation and short residence time involved in this process, the broken cylinders can be frozen in a metastable state before the final equilibrium is reached.

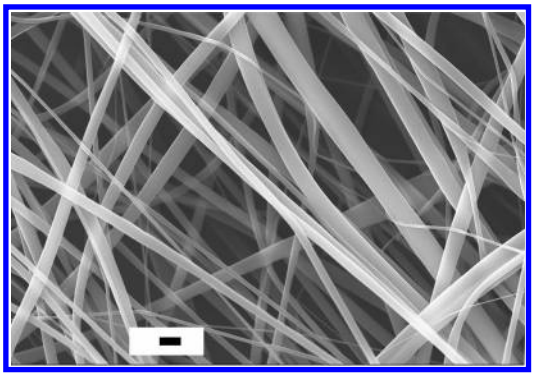

Figure 1. SEM image of electrospun IS29 PS-*b*-PI fibers from 30 wt % solution in THF. Scale bar is 3 μm.

SAXS experiments were performed on nonwoven fiber mats, and results are shown in Figure 3. The presence of a well-defined first-order peak confirms microphase separation between the two blocks. However, a weak second-order peak at a ratio of $\sqrt{3}$ indicates the presence of largely disordered morphology. For example, two different SAXS patterns for as-spun IS29 fibers taken at different regions of the same sample are shown in Figure 3. The presence of the second-order peak in only one curve shows that the electrospun fibers have regions of both ordered cylindrical domains and disordered PI domains in the PS matrix. It is also worth noting that the *d* spacing between isoprene cylinders is smaller in fibers than in films. A similar reduction in *d* spacing was seen by Pakula et al.,[24] who studied the elongational deformation behavior of styrene−butadiene−styrene triblock copolymer with a cylindrical morphology, while Kim et al.[27] observed the same decrease in domain spacing as the solvent evaporation rate was increased in thin films of 100 nm in thickness. The decrease in *d* spacing from the equilibrium bulk value in our system could be a combined effect of both extensional deformation and rapid solvent evaporation.

To investigate the effect of annealing on domain structures, electrospun fibers were annealed at 80 °C for 24 and 48 h. The TEM image of a longitudinal cross section of 24 h annealed fiber is shown in Figure 2c. The annealed fiber shows some evidence of longer cylinders with a tendency to align along the fiber axis. Because of the confinement of the fiber curvature, the PI domains are not able to reorient themselves completely, and a substantial annealing effect on structure development is seen in the SAXS data only at a temperature of 110 °C, as shown in Figure 3. The annealing effect is seen with the emergence of a higher order peak, indicating the beginning of formation of some long-range order. Although annealing at temperatures above 90 °C also helps the external stresses imposed during electrospinning, and recover the domain spacing of the original undeformed state, fiber morphology is not fully preserved above 110 °C. The *d* spacings of both as-spun and annealed IS29 fibers at various temperatures are summarized in Table 1. It is observed

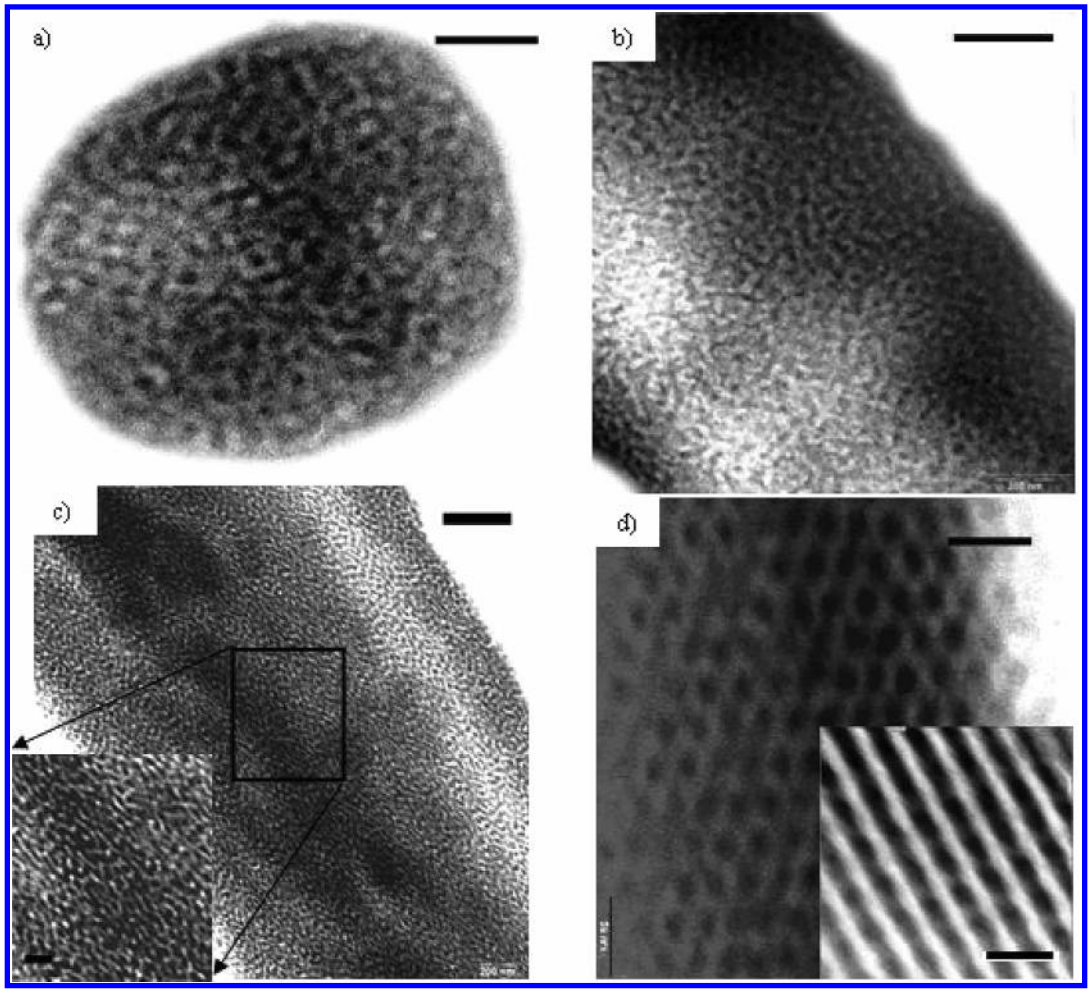

Figure 2. TEM images of IS29 system: (a) cross section of fibers spun from 30 wt % solution in THF, scale bar = 100 nm; (b) along the axis of as-spun fiber, scale bar = 200 nm; (c) along the axis of fiber annealed for 24 h at 80 °C, scale bar = 200 nm, inset scale bar = 50 nm; and (d) film cast from 10 wt % solution in THF, side view and top view scale bars = 50 nm.

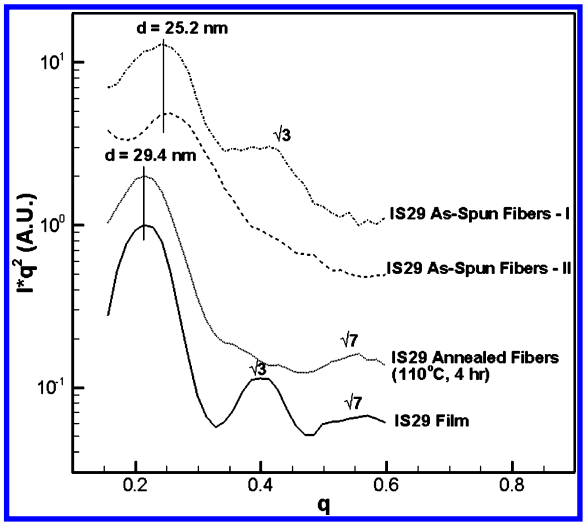

Figure 3. SAXS patterns of IS29 fibers and film. Fibers were spun using a 30 wt % solution in THF. Two different SAXS curves for as-spun IS29 fibers taken at different regions of the same sample are shown.

that the *d* spacing increases with the degree of annealing and eventually recovers that of the film.

IS53 Electrospun Fibers. Similar studies were done on IS53 copolymer. Films were cast from a 10 wt % solution in THF, and lamellar morphology was obtained via TEM and SAXS as shown in Figures 4 and 5. 15−25 wt % polymer solutions in THF were electrospun. TEM images of the cross section of fibers spun from 25 wt % IS53 copolymer in THF are shown in Figure 4. We find two different morphologies in as spun fibers (Figure 4a,b). While we see alternating parallel layers of PI and PS at the edges of the fiber cross section in one type of morphology (Figure 4a), we find some evidence of alternating segments of PI and PS in the other with PI located at the outer walls due to its lower surface energy (Figure 4b). However, both morphologies show disordered PI domains in the center of the cross section due to high deformation rates and short residence time during electrospinning. The domain spacing of fibers is substantially lower than that of the film. One possible explanation for this is the strong confinement and curvature effect of the fiber morphology due to the relatively large equilibrium domain spacing of high molecular weight IS53 copolymer. This along with the other effects of elongation and rapid solvent evaporation causes a compression of the lamellar morphology. However, the reason for such a small domain spacing in fibers is still not well understood.

Table 1. Domain Spacing Obtained for IS29 Fibers on Annealing at Various Temperatures

	as-spun fibers	80 °C, 24 h	100 °C, 4 h	110 °C, 4 h	film
d spacing (nm)	25.2	25.2	27.6	29.4	29.4

We annealed the IS53 fibers at 90 °C for 12 h, and TEM images of fiber cut across the cross section and along the fiber axis are shown in parts c and d of Figure 4, respectively. Only

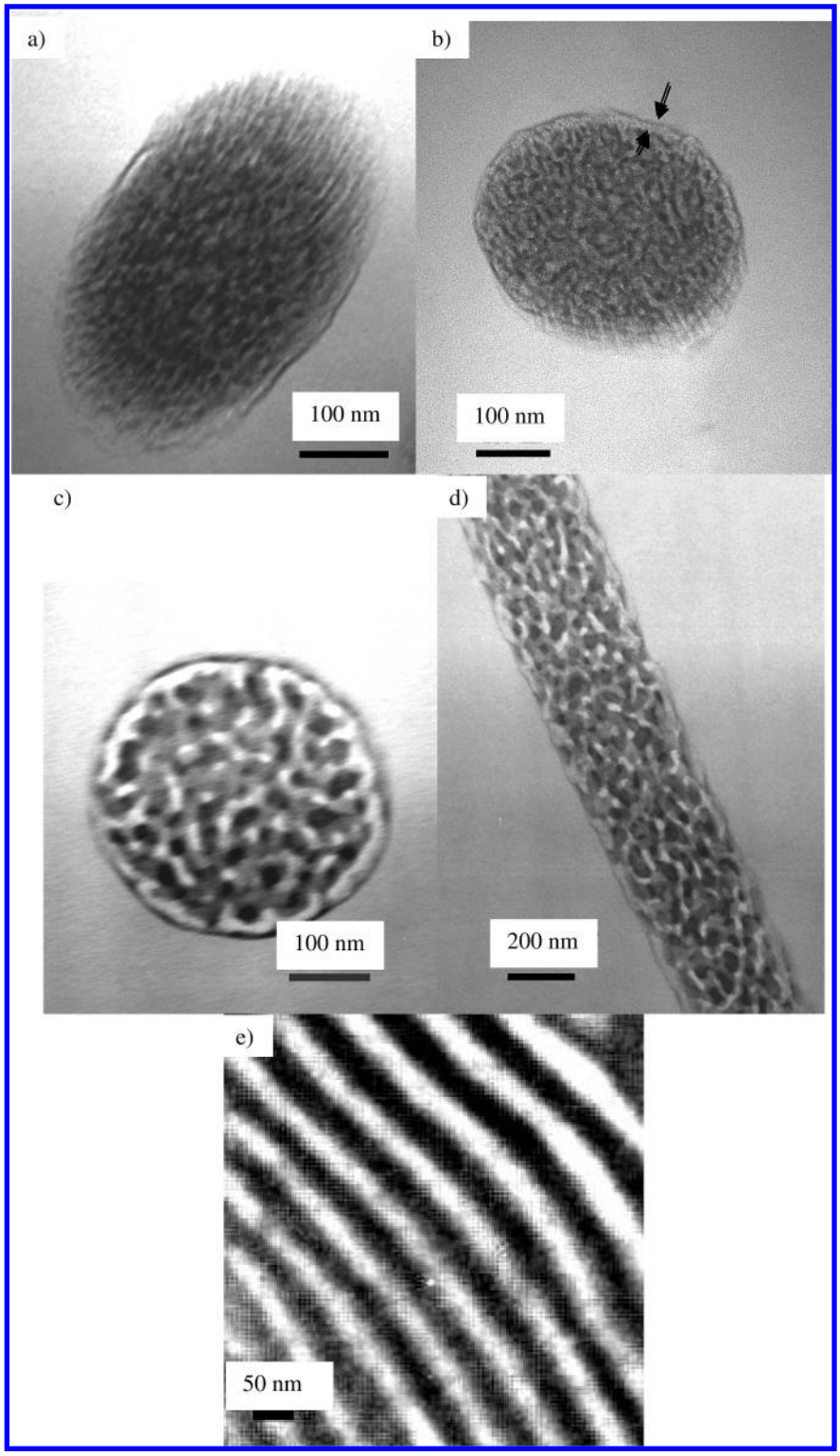

Figure 4. TEM images of IS53 copolymer: (a, b) two cross sections with different domain structures of fiber spun from 25 wt % solution in THF; (c) cross section of fiber annealed at 90 °C for 12 h; (d) along the axis of fiber annealed at 90 °C for 12 h; (e) film cast from 10 wt % solution in THF.

one kind of morphology which shows the emergence of alternating concentric rings of PI and PS with PI on the outer walls was found in the annealed fibers. In addition, the annealed fibers show a better contrast between the blocks, indicating stronger segregation. However, the morphology is still largely disordered in the center. The TEM image along the fiber axis shows small broken domains again due to high extensional deformation during electrospinning. SAXS experiments were performed on IS53 fiber mats, and results are shown in Figure 5. Again, the presence of a well-defined first-order peak confirms microphase separation between the two blocks. However, no clear second-order peak in as-spun fibers indicates the presence of largely disordered morphology as in the IS29 system. It is also observed that the *d* spacing between isoprene domains is smaller in fibers than in films. SAXS experiments were done on IS53 electrospun fibers annealed at 100 °C for 12 h. The annealing effect is seen with the emergence of a higher order peak, indicating the beginning of formation of some long-

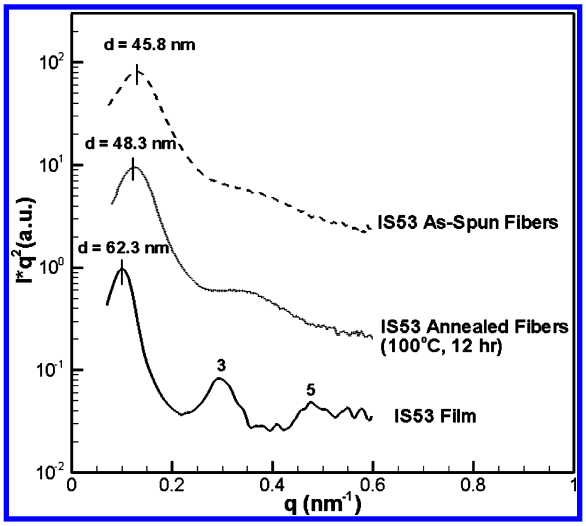

Figure 5. SAXS patterns of IS53 fibers and film. Fibers were spun using a 25 wt % solution in THF.

range order, but the PI domains are not able to reorient themselves completely possibly due to the confinement of the fiber curvature. Annealing at 100 °C for 12 h gives rise to only a small increase in the domain spacing which is still substantially lower than the bulk repeat period.

Conclusion

We have presented evidence of microphase separation such as cylindrical and lamellar morphology in electrospun PS-*b*-PI nanofibers via TEM and SAXS studies. However, the domains in electrospun fibers are not well ordered due to the fast solvent evaporation and strong elongational deformation involved in the electrospinning process. IS29 fibers show smaller domain spacing than the corresponding film. However, the microdomains relax back to their equilibrium spacing on annealing. For IS53 copolymer, the bulk repeat period is very large due to its high molecular weight, making the effect of cylindrical confinement due to fiber morphology substantial. This leads to an extremely small domain spacing in fibers as compared to the IS53 film. Although the *d* spacing increases on annealing these fibers, it is not able to relax back to its equilibrium. A comprehensive annealing study at different temperatures and various time ranges to obtain more uniform microdomain structures for both cylindrical and lamellar morphology is underway.

Acknowledgment. This work was supported by NanoteK Consortium in Kraft Foods, and the Cornell Center for Materials Research (CCMR), a Materials Research Science and Engineering Center of the National Science Foundation (DMR-0079992). The authors thank Sol Gruner for the use of the SAXS facility.

References and Notes

(1) Fong, H.; Reneker, D. H. In *Structure Formation in Polymeric Fibers*; Salem, D. R., Ed.; Hanser Gardner Publications: Munich, 2001.
(2) Dzenis, Y. *Science* **2004**, *304*, 1917.
(3) Li, B. D.; Xia, Y. *Adv. Mater.* **2004**, 16, 1151.
(4) Casper, C. L.; Stephens, J. S.; Tassi, N. G.; Chase, D. B.; Rabolt, J. F. *Macromolecules* **2004**, *37*, 573.
(5) Fong, H.; Liu, W.; Wang, C. S.; Vaia, R. A. *Polymer* **2002**, *43*, 775.
(6) Zhou, H.; Kim, K. W.; Giannelis, E. P.; Joo, Y. L. In *Polymeric Nanofibers*; ACS Symp. Ser. Book Vol. 198; American Chemical Society: Washington, DC, 2006.
(7) Fong, H.; Reneker, D. H. *J. Polym. Sci., Part B* **1999**, *37*, 3488.
(8) Ma, M.; Hill, R. M.; Lowery, J. L.; Fridrikh, S. V.; Rutledge, G. C. *Langmuir* **2005**, *21*, 5549.
(9) Ruotsalainen, T.; et al. *Adv. Mater.* **2005**, *17*, 1048.
(10) Khandpur, A. K.; et al. *Macromolecules* **1995**, *28*, 8796.
(11) Bates, F. S.; Fredrickson, G. H. *Annu. Rev. Phys. Chem.* **1990**, *41*, 525.
(12) Matsen, M. W.; Schick, M. *Phys. Rev. Lett.* **1994**, *72*, 2660.
(13) Fredrickson, G. H.; Bates, F. S. *Annu. Rev. Mater. Sci.* **1996**, *26*, 501.
(14) Almdal, K.; Koppi, K. A.; Bates, F. S.; Mortensen, K. *Macromolecules* **1992**, *25*, 1743.
(15) Park, C.; Yoon, J.; Thomas, E. L. Polymer **2003**, *44*, 6725.
(16) Sota, N.; Hashimoto, T. *Polymer* **2005**, *46*, 10392.
(17) Hoffman, A.; Sommer, J.; Blumen, A. *J. Chem. Phys.* **1997**, *106*, 6709.
(18) Fraser, B.; Denniston, C.; Muser, M. H. *J. Polym. Sci., Part B* **2005**, *43*, 970.
(19) Srinivas, G.; Discher, D.; Klein, M. L. *Nat. Mater.* **2004**, *3*, 638.
(20) Groot, R. D.; Madden, T. J.; Tildesley, D. J. *J. Chem. Phys.* **1999**, *110*, 9739.
(21) Hamley, I. W. *J. Phys.: Condens. Matter* **2001**, *13*, 643.
(22) Harada, T.; Bates, F. S.; Lodge, T. *Macromolecules* **2003**, *36*, 5440.
(23) Seguela, R.; Homme, J. P. *Macromolecules* **1981**, *14*, 197.
(24) Pakula, T.; Saijo, K.; Kawai, H.; Hashimoto, T. *Macromolecules* **1985**, *18*, 1294.
(25) Shin, K.; Xiang, H.; Moon, S. I.; Kim, T.; McCarthy, T. J.; Russel, T. P. *Science* **2004**, *306*, 76.
(26) Daniel, C.; Hamley, I. W.; Mortensen, K. *Polymer* **2000**, *41*, 9239.
(27) Kim, G.; Libera, M. *Macromolecules* **1998**, *31*, 2569.

MA052643A